THE BELL SYSTEM

TECHNICAL JOURNAL

DEVOTED TO THE SCIENTIFIC AND ENGINEERING
ASPECTS OF ELECTRICAL COMMUNICATION

Volume 52 March 1973 Number 3

The Elimination of Tuning-Induced Burnout and Bias-Circuit Oscillations in IMPATT Oscillators

By C. A. BRACKETT

(Manuscript received August 18, 1972)

IMPATT diode microwave oscillators suffer from the effects of low-frequency instabilities, which include excessive up-conversion of bias-circuit noise, bias-circuit oscillations, and diode burnout induced by tuning at the microwave frequency. These instabilities are particularly troublesome in GaAs diodes, although also present in both Ge and Si to a lesser extent. Moreover, these instabilities are more prominent in higher efficiency, higher power diodes, presenting a severe systems problem in the practical utilization of GaAs diodes at their highest power and efficiency levels. In this paper, it is shown that these instabilities may be eliminated in a systematic and well controlled manner with little or no loss in microwave power or efficiency.

It is shown that the source of the unstable behavior is a low-frequency RF voltage-induced negative resistance which extends from dc to several tens, and perhaps hundreds, of megahertz, depending on the loaded Q of the microwave circuit. The negative resistance is an unavoidable fact of large-signal avalanche diode operation and is due to the rectification properties of the nonlinear microwave avalanche. Experiments are performed in which the negative resistance and its associated inductive reactance are

measured as functions of the dc bias current, baseband frequency, and microwave circuit loading and Q.

An analysis is performed and a simple small-signal equivalent circuit is derived for the diode terminal impedance which yields quantitative and qualitative understanding of the interaction of the IMPATT device with the microwave oscillator circuit.

Using the equivalent circuit and experimental characterization, a stability criterion is developed that is simply applied to any diode-circuit combination. Using this criterion, several examples of common configurations are investigated, including the maximum shunt capacity permissible in the bias circuit for stable operation, and the effects of line length in the bias circuit. Also discussed are two means of achieving stable operation, both of which have been tested experimentally and shown to work.

The scaling laws are derived in an approximate manner and used to show that diodes designed for higher frequencies will have less induced negative resistance. Thus, mm-wave silicon IMPATTs would have less trouble with low-frequency instabilities than those designed at 6 GHz.

I. INTRODUCTION

Low-frequency instabilities including noise, bias-circuit oscillations, and diode burnout at low bias currents are often encountered when tuning high-power, high-efficiency IMPATT diodes. Gallium arsenide IMPATTs, which produce high power at higher efficiency and lower noise than either silicon or germanium IMPATTs, are particularly prone to these instabilities. Microwave tuning operations in GaAs often burn out diodes at bias currents of one-half to one-quarter their thermally expected values. This problem has been so serious that it has cast doubt on the practicality of using GaAs IMPATTs at their fullest potential power and efficiency. These instabilities also make the testing and evaluation of diodes a very tedious procedure and cause the operating conditions of the oscillator to be very sensitive to microwave and bias-circuit load conditions.

The cause of these problems is an RF voltage-induced negative resistance in the IMPATT diode. This negative resistance has a low-pass frequency dependence, extending from essentially zero frequency up through several tens, and perhaps hundreds, of megahertz. The upper frequency limit is determined by the bandwidth of the microwave circuit. The magnitude and frequency dependence of the induced negative resistance are dependent on the microwave circuit tuning. It is possible to tune through very high values of negative resistance,

even at low dc bias currents. If this negative resistance is not stabilized, the results can be an excess amount of upconverted microwave noise, bias-circuit oscillations, or diode burnout due to the instability achieving an excessive amplitude. Stabilization removes the instability and eliminates these "tuning-induced" burnouts, as well as the excess noise and bias-circuit oscillations.

In this paper we (*i*) discuss the physical origins of this negative resistance, (*ii*) develop an equivalent circuit which agrees with experimental observations, (*iii*) present an experimental characterization of the effect, and (*iv*) discuss the principles and techniques of stabilization which have been used experimentally to remove the instabilities.

The written history of bias-circuit design is almost nonexistent, inasmuch as very little has been known about the low-frequency impedance of IMPATT diodes. The existence of a low-frequency negative resistance effect was observed by Clorfeine and Hughes,[1] and they correctly suggested that this was induced by large RF voltages through a rectification effect and postulated that it was the cause of bias-circuit oscillation problems. They did not offer any analytic description of the effect, nor did they present a systematic characterization of it.

The construction of bias circuits has been done rather empirically, with the understanding that higher-impedance bias circuits give less upconverted noise and bias-circuit oscillations. Olson[2] disclosed the use of a resistor in the center conductor of a coaxial cavity to lower noise and remove instabilities, and others have used transistor amplifiers to raise the bias-circuit impedance. Typical examples of bias-circuit instabilities are given in an Application Note[3] published by Hewlett-Packard, along with a discussion of typical bias-circuit designs that they have used in silicon IMPATT oscillator circuits.

The rectification effect itself was contained in Read's original proposal,[4] and it has appeared in several large-signal analyses since then. What has been missing is a simple picture of how the microwave circuit completes the feedback loop to provide negative resistance and a more definite link between this negative resistance, bias oscillations, and tuning-induced burnouts.

The equivalent circuit and experimental characterization of this work permit the elimination of tuning-induced burnout, bias oscillations, and excessive noise upconversion in a straightforward manner.

Outlining the paper, in Section II, the link between burnout, bias oscillation, and negative resistance is discussed. In Section III, the physical origins are discussed and a simple analysis is given, demonstrating reasonable agreement with experiment. In Section IV, the

experimental characteristics of the total terminal impedance of the diode are given as functions of the bias current, baseband frequency, and microwave loading conditions. A small-signal equivalent circuit of the diode's terminal impedance is derived in Section V which is simple, yet describes in detail the role played by the microwave circuit. Stabilization, the elimination of the instabilities, is discussed in Section VI, giving the principles, some examples, and possible techniques. Approximate scaling rules are derived in Section VII.

Section VIII presents a summary of the paper and its major conclusions in a form complete enough to give the more casual reader a good understanding of the negative resistance mechanism and its stabilization.

II. BURNOUT AND BIAS-CIRCUIT OSCILLATION

Before proceeding with consideration of the negative resistance itself, it may be valuable to establish a link between the existence of a negative resistance, bias-circuit oscillations, and tuning-induced burnout. As described later in this paper, a negative resistance has been measured and found to exist in the circuit used at frequencies from essentially dc up to several tens of MHz. Such a negative resistance may act as an amplifier of bias-circuit noise, resulting in a modulation of the oscillator amplitude and frequency and producing the upconversion of large amounts of noise to the microwave frequency. Under certain conditions, the bias circuit may break into sustained oscillations producing a combined AM and FM spectrum about the microwave signal. When either of the above events occurs (excessive noise upconversion or bias-circuit oscillation), there is grave danger of burning out the diode. Specifically, it is found that

(*i*) without stabilization of the negative resistance, low-current burnouts are frequent,
(*ii*) bias-circuit noise and/or oscillations accompany or precede the burnout,
(*iii*) stabilization of the negative resistance removes the noise and the bias-circuit oscillations, and stops the low-current burnouts,
(*iv*) the microwave tuning conditions likely to produce burnouts are the same as those that produce the noise and bias oscillations.

Thus, circumstantial evidence strongly links the negative resistance, the bias-circuit oscillations, and the low-current tuning-induced burnouts to each other. A specific sequence of events leading to burnout

is not postulated. Indeed, many such sequences can be visualized. Preliminary scanning electron microscope photographs indicate no difference between pure thermal (nonoscillating) burnouts and low-current tuning-induced burnouts. Both have the same characteristic gold fingers shorting out the junction that were first described by Evans, et al.[5]

III. PHYSICAL ORIGINS OF THE NEGATIVE RESISTANCE

The three essential ingredients which cooperate to produce the low-frequency negative resistance are

(*i*) a large-signal rectification effect wherein the dc voltage (at constant current) is lowered by an increase in the microwave voltage amplitude,

(*ii*) the dependence of the diode's microwave conductance, $g_d(V_a,I_d)$, upon the microwave voltage amplitude, V_a, and the dc bias current, I_d, and

(*iii*) the microwave circuit constraint

$$g_d(V_a,I_d) + G(\omega) = 0$$

where $G(\omega)$ is the microwave circuit conductance into which the diode oscillates. The first of these, the rectification effect, is summarized by Read[4] in the equation (for the Read diode)

$$V_d = \frac{W\tau}{2\epsilon A} I_d - \frac{m}{4WE_c} V_a^2 + \text{constant} \tag{1}$$

where

V_d = dc voltage,

W = depletion layer width,

τ = drift zone transit time,

ϵ = dielectric constant,

A = junction area,

$m = (E/\alpha)(d\alpha/dE)\,|_{E_c}$ = percentage change in the avalanche coefficient α for a percentage change in the electric field, and

E_c = critical field for avalanche breakdown.

Equation (1) is approximate, neglecting higher powers of V_a. Studies made with the nonlinear program introduced by Blue,[6] however, indicate that (1) is an excellent approximation.

The net dc terminal resistance from (1) is then

$$R_t = \frac{dV_{dc}}{dI_d} = R_{sc} - \frac{mV_a}{2WE_c}\frac{dV_a}{dI_d} \tag{2}$$

where $R_{sc} = W\tau/2\epsilon A$ is the space-charge resistance.

From the microwave circuit constraint, we see that the ac voltage amplitude V_a and the dc bias current I_d are [for fixed $G(\omega)$] not independent of each other. In fact,

$$\frac{dV_a}{dI_d} = -\frac{\left(\frac{\partial g_d}{\partial I_d}\right)_{V_a}}{\left(\frac{\partial g_d}{\partial V_a}\right)_{I_d}}. \tag{3}$$

In the usual situation $(\partial g_d/\partial I_d)_{V_a} < 0$ and $(\partial g_d/\partial V_a)_{I_d} > 0$ (remembering that g_d is itself negative), so $(dV_a/dI_d) > 0$ and the last term of (2) represents a negative resistance. It is this negative resistance which causes the instabilities in the bias circuit. It is associated, basically, with amplitude modulation of the microwave oscillation. The rectification property is due to the nonlinearity of the avalanche process whereby a sinusoidal field variation about the critical field, E_c, produces many more charges on the positive swing than it does on the negative. This means that either the dc current increases, or the dc voltage drops, as the RF voltage increases.

A simple picture then is as follows. A positive fluctuation of the diode current increases the microwave negative conductance (in magnitude). This causes the voltage amplitude, V_a, to increase in order to meet the circuit constraint, and the increase in V_a requires a drop in the dc voltage, thereby creating negative resistance.

Equation (2) can be written

$$R_t = R_{sc} - \frac{m}{2WE_c}\frac{1}{G}\frac{dP_{\text{out}}}{dI_d} \tag{4}$$

where G is the microwave circuit conductance at the oscillation frequency and P_{out} is the microwave output power. This form is convenient because G can be estimated and dP_{out}/dI_d can be easily measured in any particular circuit. Doing this, and using published data for the other constants, R_t has been calculated for typical silicon, germanium, and gallium arsenide IMPATT diodes designed to operate at 6 GHz. This data is shown in Table I and it indicates reasonable agreement with the experimental values also shown. Silicon has the

TABLE I—PHYSICAL DATA AND NEGATIVE RESISTANCE VALUES FOR SILICON, GERMANIUM, AND GALLIUM ARSENIDE IMPATTS

	Si	Ge	GaAs	Source
$C_{\text{Breakdown}}$ (pF)	~0.7	~0.7	2.5	Measured
$V_{\text{Breakdown}}$ (volts)	105	45	95	Measured
W (microns)	5	4	4	Ref. 7, p. 117
E_c (volts/cm)	3.5×10^5	2.1×10^5	6.5×10^5	Ref. 7, p. 117
$\frac{E_c}{\alpha}\frac{d\alpha}{dE}\Big\vert_{E_c}$	5.0	6.1	19.5	Calculated
$\frac{dP_{\text{out}}}{dI_d}$ (watts/amp)	13.6	10	24.4	Measured
G (mhos)	3×10^{-3}	3×10^{-3}	6×10^{-3}	Estimated[8]
R_- (ohms)	65	117	152	
R_{sc} (ohms)	25	59	25	Calculated
Theoretical R_t (ohms)	−40	−58	−127	Calculated
Experimental R_t (ohms)	−12	−50	−122	Measured

smallest negative resistance and the largest discrepancy between theory and experiment. Germanium has about (−)50 ohms of induced negative resistance, indicating that difficulties might be encountered if biased through a 50-ohm bias line. The gallium arsenide results indicate about (−)120 ohms induced negative resistance. Measured values have been everywhere between (−)85 ohms and (−)150 ohms. On the basis of this data alone, it would be expected that biasing GaAs diodes would be very difficult.

A complete experimental characterization of the low-frequency impedance is given in the next section.

IV. EXPERIMENTAL CHARACTERIZATION

The technique used to measure the low-frequency impedance of the diode was to induce bias-circuit oscillations and to barely quench them by adjusting the bias-circuit impedance. Then the diode was removed from the circuit and the impedance of the circuit as seen by the diode was measured at the frequency of the bias-circuit oscillation. The quenching impedance, Z_Q, measured in this way, is the negative of the small-signal impedance of the diode, Z_t, and could be measured as a function of the bias-circuit oscillation frequency, the microwave loading, and the bias current. The microwave frequency of oscillation was always tuned to that for maximum power output.

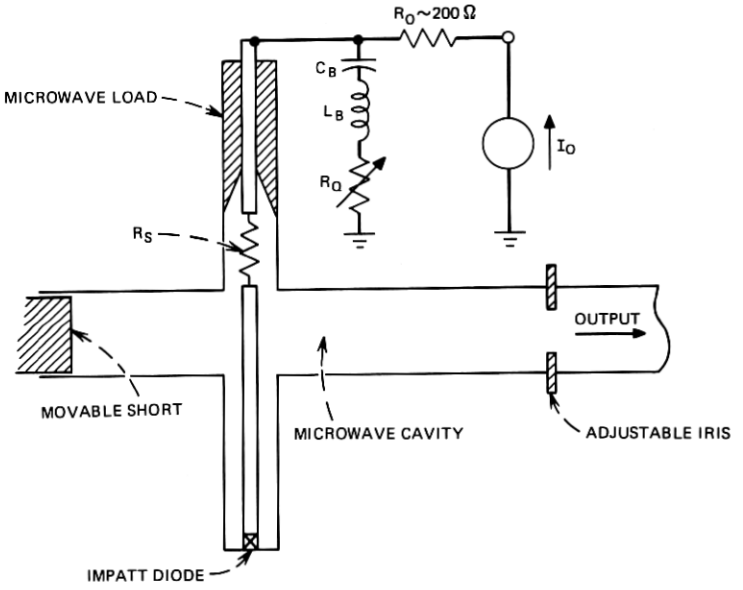

Fig. 1—Microwave cavity and bias configuration. The IMPATT diode is mounted at the end of a coax line which is coupled to the microwave cavity. The bias circuit includes a stabilizing resistor R_s, a resonant circuit C_B, L_B, R_Q used to induce bias-circuit oscillations, and a resistor R_o to isolate the bias circuit from the constant current supply I_o.

In order to perform this experiment, it was necessary to use an oscillator and bias circuit with the following two properties: (*i*) a bias circuit which could be made stable or unstable at all values of current and microwave loading, and (*ii*) microwave loading which could be varied continuously from above oscillation threshold down to zero external loading. A suitable circuit is one described by Magalhaes and Kurokawa[9] and illustrated in Fig. 1. It consists of a waveguide microwave cavity coupled to a coaxial transmission line. The waveguide cavity is formed between a movable short and an adjustable iris, which is used to couple the cavity to the output waveguide load. The adjustable iris is formed by rotating the rectangular waveguide cavity with respect to the output rectangular waveguide at a flanged joint.

The diode is situated at one end of the coaxial line (its distance from the waveguide was adjustable for tuning purposes) and the coaxial line is terminated on the opposite side of the cavity from the diode in a microwave load. The microwave load is an open circuit to dc and may be represented as a shunt capacitance of about 35 pF at bias-

circuit frequencies. The dc bias is fed in through the coaxial line from a constant-current supply. An isolation resistor of about 200 ohms was used to reduce the effects of the parasitic reactances of the power supply and its leads on the bias-circuit impedance. It was found that placing a series resistance R_s (2-watt carbon resistor) in the bias line would stabilize the induced negative resistance formed in the diode. A value of $R_s = 150$ ohms was sufficient to stabilize the diode at all bias currents up through the thermal limit of the resistor R_s and at all microwave loading levels.

The bias oscillation was induced by reducing R_s and adding a shunt resonant circuit with a quenching resistor R_Q. The resonant circuit

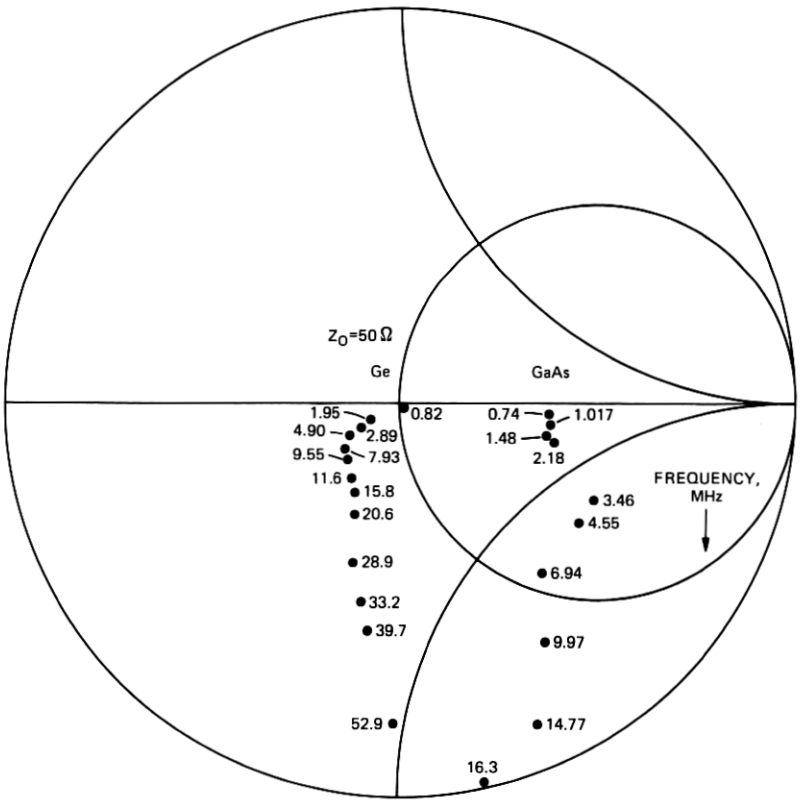

Fig. 2—Quenching impedance versus frequency of bias-circuit oscillations for Ge and GaAs measured at the diode's terminals. Bias currents were 100 mA and 120 mA for Ge and GaAs respectively. The quenching impedance is the negative of the diode's small-signal impedance, indicating a negative resistance and inductive reactance.

was used to tune the bias oscillation to the desired frequency and it was brought to the quenched, or small-signal, level by adjusting R_Q. Measuring the circuit impedance with the diode removed then gave the desired measurement of Z_Q.

The result of such a procedure at constant bias current and constant microwave loading conditions is shown in Fig. 2 for typical 6-GHz Ge and GaAs diodes. Since $Z_t = -Z_Q$, we see from Fig. 2 that the diode impedance has a general low-pass characteristic for the negative real part, becoming positive at frequencies higher than some frequency f_M. It is also seen that the reactive part of Z_t is inductive. This general character to Z_t has been observed in all diodes upon which these measurements have been made. The frequency f_M is the maximum frequency at which the bias circuit can be made to oscillate and is dependent upon the loaded Q of the microwave circuit, as will be explained in Section V. The scatter in the data from smooth contours is probably due to the difficulty of obtaining identical microwave tuning on successive measurements. The general range of low-frequency asymptotes for R_t for GaAs was from $(-)85$ ohms to $(-)150$ ohms. For Ge this range was from $(-)35$ ohms to $(-)75$ ohms, although less data is available for the Ge diodes. These experiments have been attempted on Si 6-GHz IMPATTs as well, with the results indicating

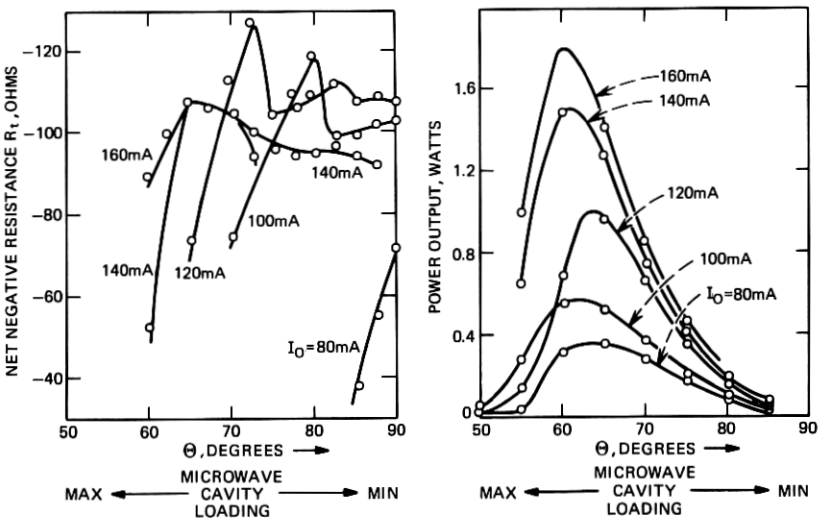

Fig. 3—Output power and induced net small-signal negative resistance as a function of bias current and microwave loading for GaAs. Microwave frequency was 4.7 GHz, bias-circuit frequency was ~5 MHz.

a maximum observed negative resistance of about (−)20 ohms. However, with the microwave circuit tuned to best overall operation, these 6-GHz Si diodes would not sustain bias-circuit oscillation, but only emit large amounts of baseband noise as the bias-circuit impedance was lowered. This is explained in Section V, where the equivalent circuit of this impedance is developed.

In Fig. 3, the small-signal-induced negative resistance, R_t, is shown as a function of bias current and microwave loading. This data was all taken at a bias-oscillation frequency of ~5 MHz. Also shown is the output power. The microwave loading is changed by rotating the output waveguide relative to the cavity waveguide, the angle between them denoted by Θ. For $\Theta \rightarrow 0$, the guides are aligned and the microwave cavity has its maximum loading, which implies zero (or at least minimum) microwave voltage amplitude. Increasing the rotation Θ, one passes through oscillation threshold to maximum power output and finally to maximum oscillation amplitude and zero output power in the minimally loaded condition. Thus, Θ may be considered to be an indication of microwave voltage amplitude or microwave load conductance. From Fig. 3 we make the following observations.

(*i*) At low bias currents, the negative resistance is small at normal maximum power loading conditions, but does become significant at the lightest loading ($\Theta \rightarrow 90$ degrees).

(*ii*) The negative resistance increases rapidly with bias current until it saturates at a level around (−)120 ohms (for this diode). Further increases in current tend only to translate the maximum negative resistance toward greater microwave loading conditions (smaller Θ), with the result that, at 160 mA, the loadings for maximum power and maximum induced negative resistance are nearly coincident.

(*iii*) There appears to be considerable structure to the negative resistance curves. This structure appears to be real because a decrease in either the current or the angle Θ from the condition $I_o = 140$ mA, $\Theta = 75$ degrees results in an increased amplitude of oscillation and sometimes burnout of the diode.

The reason the negative resistance increases with current at low currents and increases with Θ at the lower Θ is presumably associated with an increase of the voltage V_a. The apparent saturation of the negative resistance at higher currents and larger Θ is not understood. It may be associated with a saturation of the RF voltage V_a, or more

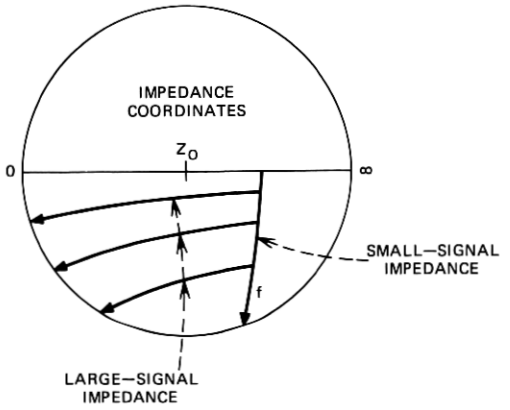

Fig. 4—Schematic illustration of the negative of the small-signal and large-signal diode impedance at bias-circuit frequencies. The large-signal impedances move in the direction of decreasing negative resistance with increasing bias oscillation amplitude.

likely with the detailed dependence of the diode's microwave admittance, y_d, on V_a and I_d at high V_a and high I_d.

One further experimental characteristic is that, if the bias oscillation is allowed to rise above the quenching level, the real part of Z_Q decreases as shown schematically in Fig. 4. This implies that the device impedance Z_l is open-circuit stable and is properly characterized as a negative resistance. It also explains the well-known fact that high-impedance termination of the bias circuit lowers the AM noise significantly.[10] Since the negative resistance acts as an amplifier of noise in the bias circuit, the lower the circuit impedance, the higher the gain and the larger the noise modulation of the microwave power become. In the following section, the small-signal equivalent circuit is worked out in detail and most of the observed features are explained on theoretical grounds.

The open-circuit stability and large-signal characteristics have a profound significance as to the elimination of both bias-circuit oscillations and diode burnout, as will be discussed at length in Section VI.

V. LOW-FREQUENCY EQUIVALENT CIRCUIT

It is evident by now that the microwave oscillator circuit plays an important role in the existence of the low-frequency negative resistance. The question arises, however, as to the role it plays in determining the bandwidth and magnitude of the negative resistance and why the reactance associated with R_l is always inductive. In this section

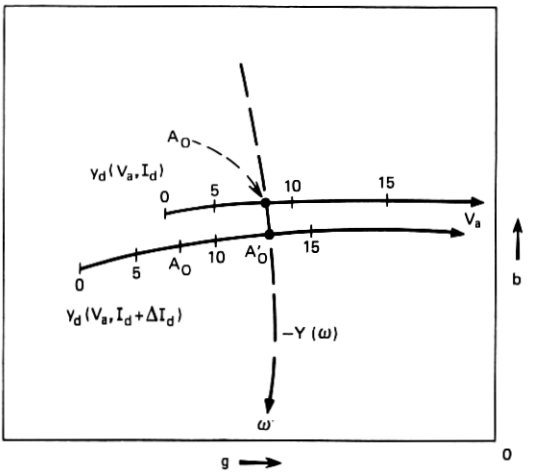

Fig. 5—Schematic admittance-plane description of the microwave large-signal device admittance, $y_d(V_a,I_d)$, and the negative of the microwave circuit admittance, $-Y(\omega)$. The intersection of y_d with $-Y$ determines the amplitude of the microwave oscillation A_o and the frequency ω. An increase in I_d requires an increase in V_a from A_o to A'_o as shown.

an equivalent circuit is developed, on an analytical basis, which fits the data of the previous section, and is used further in Section VI to consider the problems of stabilization.

To develop the equivalent circuit, a quasi-static model is used in which it is assumed that the diode's microwave admittance, $y_d(V_a,I_d)$, is an instantaneous function of V_a and I_d. For example, a sudden change in the dc bias current is assumed to shift the entire large-signal diode characteristic as shown in Fig. 5 from $y_d(V_a,I_d)$ to $y_d(V_a, I_d + \Delta I_d)$. Because of the large amount of energy stored in the microwave circuit, however, the RF voltage V_a cannot change instantaneously. Therefore, immediately after the change in bias current, the circuit constraint $y_d(V_a,I_d) + Y(\omega) = 0$ is not satisfied and can only be satisfied by the growth of V_a from $V_a = A_o$ to a new value A'_o as shown in Fig. 5. Such growth takes time and the amount of delay is related to the bandwidth of the microwave cavity. We can easily imagine that, if I_d were to fluctuate rapidly enough, faster than the circuit can respond, then V_a would maintain its average value and the induced negative resistance would disappear.

Using the quasi-static approach mentioned, the low-frequency (baseband) impedance, Z_t, of an IMPATT diode is derived in the

Appendix. It is found that

$$Z_t = R_{sc} - \frac{R_-}{1 + j\omega/\gamma} \tag{5}$$

with the definitions

$$R_- = \frac{m}{4WE_c} \frac{\sin \chi}{\sin \theta} \left| \frac{dV_a^2}{dI_d} \right| \tag{6}$$

and

$$\gamma = \frac{\sqrt{r^2 + s^2}}{\left| \frac{\partial Y}{\partial \omega} \right|} G \sin \theta . \tag{7}$$

Here, r and s are saturation parameters associated with the large-signal behavior of the diode admittance y_d as defined in eq. (17) of the Appendix, and $Y \equiv G + jB$ is the admittance of the microwave circuit. The angles χ and θ are defined in Fig. 6. In the admittance plane plot of this figure, $-Y(\omega)$ is the locus of the *negative* of the microwave circuit admittance in the neighborhood of the oscillation frequency ω_o; the arrow indicates the direction of increasing frequency. The large-signal admittance of the diode at frequency ω_o is assumed to intersect the $-Y(\omega)$ locus at the point P, which in fact determines the oscillation amplitude, V_a, and the frequency, ω_o. The line $y_d(V_a)$ indicates

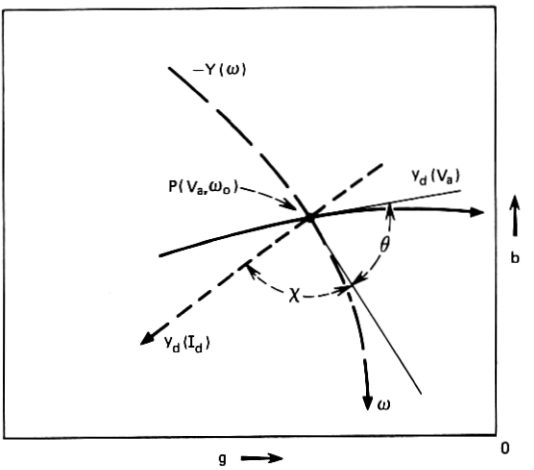

Fig. 6—Illustrating the definitions of the angles θ and χ at the intersection of the device admittance $y_d(V_a)$ and the circuit admittance $-Y(\omega)$. The intersection angle is θ for microwave voltage variations and is χ for bias-current variations. The angle $\theta + \chi$ is determined by the device alone.

the direction of the admittance plane in which the diode's admittance moves for increased voltage, V_a, at constant current. The line $y_d(I_d)$ is likewise the direction in which the diode's admittance moves for increased I_d at constant oscillation amplitude, V_a. The angles θ and χ give the intersection angles of $y_d(V_a)$ and $y_d(I_d)$ with the locus $-Y(\omega)$ as shown in the figure. It is well known[11] that one of the conditions for oscillation at the point P is that $0 \leqq \theta \leqq \pi$, with $\theta = \pi/2$ generally giving the best system performance (highest oscillator stability, lowest noise).

From (5) and (6) we see that at very low frequencies ($\omega/\gamma \ll 1$) and if $\sin \chi/\sin \theta = 1$ (a reasonable condition, as will be seen) then $Z_t = R_{sc} - R_-$ with R_- the same as found on a dc basis in eq. (2). We see that the space-charge resistance is a stabilizing factor, tending to lower the net negative resistance. At low enough frequencies, thermal effects become important and introduce further positive resistance. The latter is neglected here due to the relatively low cutoff frequency for thermal effects compared to γ.

Considering eq. (6) for R_-, we see that, if θ approaches either 0 or π, R_- can become very large. In fact, $\theta = \pi/2$ gives a minimum R_-, everything else being constant Intuitively, one can see why $\theta = 0, \pi$ are critical directions. For these conditions, $y_d(V_a)$ is nearly parallel to $-Y(\omega)$ and slight changes in the current I_d can cause large changes in V_a (and the frequency ω_o as well).

This dependence on θ is consistent with experimental observations. A certain set of Si diodes (6 GHz) were found not to have a large enough negative resistance to cause bias-circuit oscillations when tuned in what was considered to be the optimum manner. Detuning the cavity, however, and readjusting the power output to the same value gave very large bias-circuit oscillations with a very definite FM microwave spectrum. It is presumed that the FM is mostly due to θ being different from $\pi/2$.

Separately considered, the angle χ could be used to minimize R_- or even to make the net resistance positive. The difficulty with this is that the total angle $\theta + \chi$ is determined totally by the diode's characteristics and has nothing at all to do with the microwave circuit. The large-signal theories of Scharfetter and Gummel[12] and Blue[6] may be used to show that the angle $\theta + \chi$ is close to π over most of the useful range of diode parameters (V_a, I_d, ω_o). Comparing Figs. 5 and 6 of the paper by Gewartowski and Morris[8] confirms this conclusion experimentally, at least for the Si diode they investigated. If $\theta + \chi \cong \pi$ and $\theta \cong \pi/2$, then $\chi \cong \pi/2$ and $\sin \chi/\sin \theta \approx 1$ for best system require-

ments. This dependence of R_- on the angle χ indicates, however, that in laboratory testing (providing $\chi + \theta$ is not actually π) it should be possible to reduce the value of R_- and inhibit bias-circuit oscillations, while at the same time maintaining high power output. Experimentally, in coaxial circuits with many degrees of freedom in the tuning it is found that burnout and bias oscillations can usually be avoided by very carefully increasing the current by small increments and retuning slightly.

The parameter γ is shown in the Appendix to be one-half the 3-dB modulation bandwidth of the oscillator. γ achieves its maximum value at $\theta = \pi/2$. We therefore see from eq. (5) that the negative resistance has a low-pass characteristic and that $Re[Z_t - R_{sc}]$ has a cutoff frequency $\omega_c = \gamma$ equal to that of the microwave circuit.

The equivalent circuit of Z_t from eq. (5) is shown in Fig. 7. Z_t is inductive, but the frequency-independent representation involves a negative capacitance $-C_- = -(1/\gamma R_-)$. We note that, in accordance with the cutoff frequency mentioned above, the product $(-R_-) \cdot (-C_-) = +1/\gamma$ gives the time constant associated with the microwave oscillator bandwidth. A Smith chart plot of $(-)Z_t/R_{sc}$ for several values of R_-/R_{sc} and with $x = \omega/\gamma$ as a normalized frequency parameter is shown in Fig. 8. In this figure we see that the loci of $-Z_t/R_{sc}$ are straight vertical lines, and that the $x = \omega/\gamma$ values are obtained by drawing straight lines between the points $z = 0 - jx$ and $|z| = \infty$. For any value of R_-/R_{sc}, there exists a maximum frequency for which Z_t has a negative real part. We call this the maximum frequency of

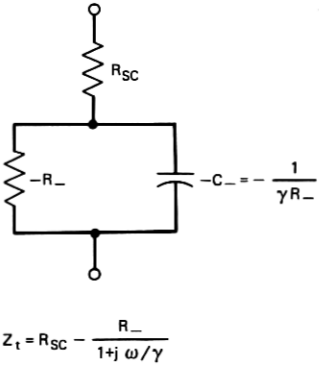

Fig. 7—Low-frequency equivalent circuit of an oscillating IMPATT diode neglecting thermal effects. R_{sc} is the space-charge resistance of the diode, γ and R_- are defined in the text.

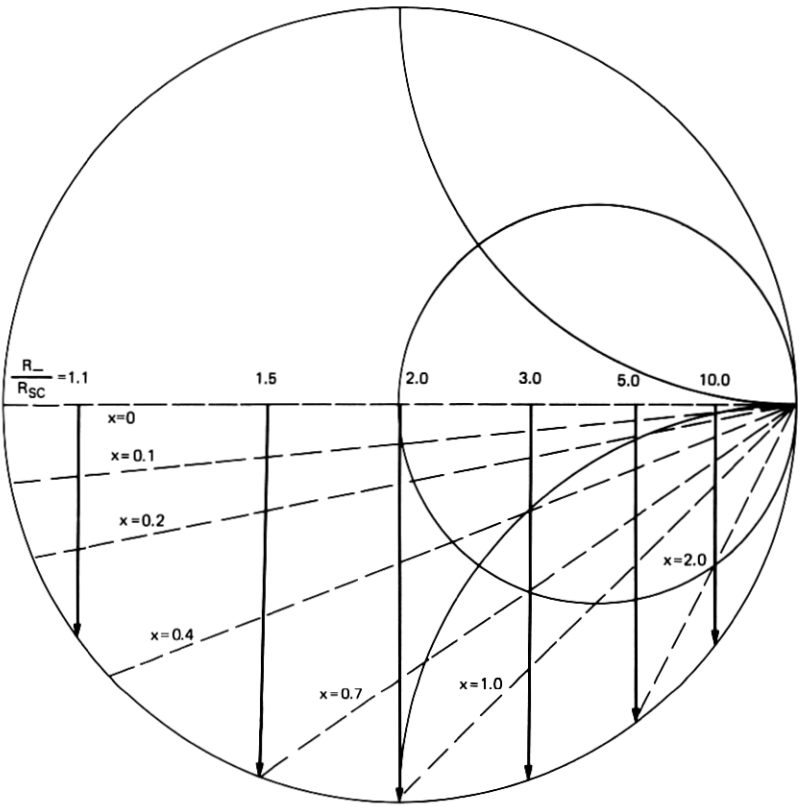

Fig. 8—The negative of the equivalent circuit impedance, Z_t/R_{sc}, normalized to the space-charge resistance, versus normalized frequency $x = \omega/\gamma$. The straight line characteristics of this plot make it useful in estimating the ratio of f_M from the values of R_-, R_{sc}, and γ.

oscillation, f_M, and it is given by

$$f_M = \frac{\gamma}{2\pi}\sqrt{\frac{R_-}{R_{sc}} - 1}. \tag{8}$$

Thus, the maximum frequency of oscillation may be greater than or less than $\gamma/2\pi$, depending on the ratio R_-/R_{sc}.

The normalization of Z_t to R_{sc} is convenient for simple construction of the loci and finding the ratio $2\pi f_M/\gamma$, but experimental results are more appropriately normalized to the bias line characteristic impedance as was done in plotting Z_Q in the previous section (Fig. 2). There are three independent parameters in the equivalent circuit for Z_t, namely,

R_-, R_{sc}, and γ. By measuring the impedance Z_t at three frequencies, one may calculate these parameters. Usually, R_{sc} can be measured in dc tests, so that only two measurements of $Z_t(\omega)$ are required. In Fig. 9, the data for the GaAs diode of Fig. 2 have been replotted along with the equivalent circuit curve obtained from the data $R_t(\omega = 0) = R_{sc} - R_- = -110\ \Omega$, $f_M \cong 17$ MHz, and $R_{sc} = 33.6\ \Omega$. The scatter in the data points is, as was mentioned before, due to the difficulty of disassembling the microwave circuit and reassembling it to the same RF conditions after every measurement. Under the circumstances, the agreement is considered to be good.

To illustrate the meaning of γ further, consider the simplest model

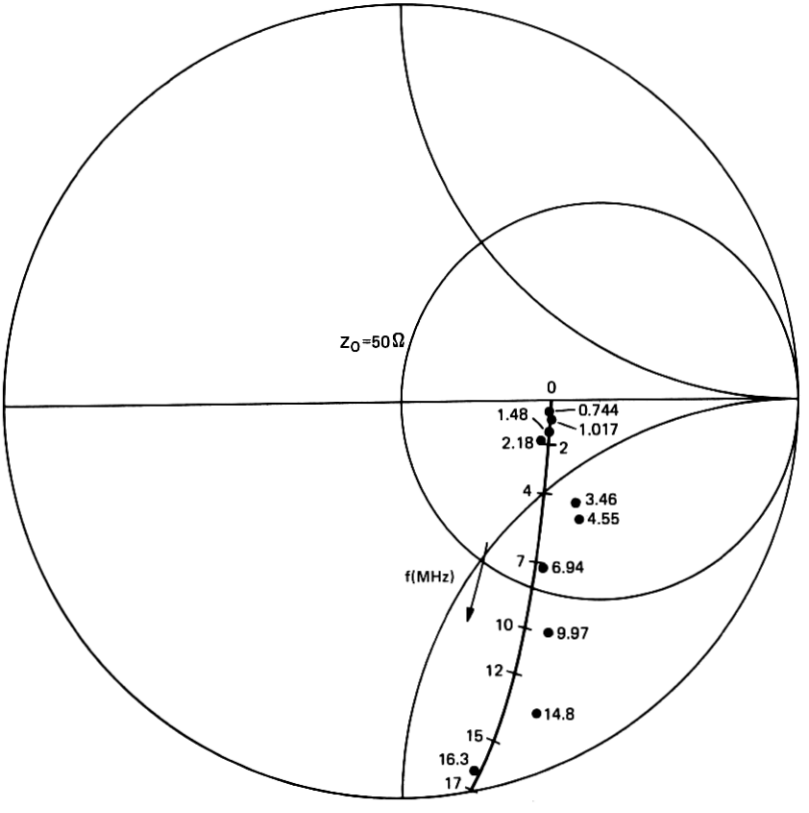

Fig. 9—Comparison of experimental (solid dots) and theoretical (solid curve) frequency dependence of the small-signal impedance Z_t. GaAs diode, $I_o = 120$ mA, $f_o = 4.7$ GHz, output power = 1 watt, $R_- = 143.6\ \Omega$, $R_{sc} = 33.6\ \Omega$, and $\gamma = 59 \times 10^6$ radians per second.

of oscillator and circuit possible in which only the diode's conductance is a function of V_a [this puts $r = 0$ in eq. (7)] and the circuit conductance does not depend upon frequency. Then eq. (7) becomes

$$\gamma = \frac{sG}{\left(\frac{\partial B}{\partial \omega}\right)} = \frac{s\omega_o}{2Q_L} \tag{9}$$

where Q_L is the loaded cavity Q. Since at maximum output power $s \cong 2$,[13] we can write under conditions for maximum power

$$\gamma \cong 2\pi \cdot \Delta f \tag{10}$$

where Δf = the full 3-dB bandwidth of the loaded cavity. Equation (8) then becomes

$$f_M = \Delta f \sqrt{\frac{R_-}{R_{sc}} - 1} = \frac{f_o}{Q_L} \sqrt{\frac{R_-}{R_{sc}} - 1}. \tag{11}$$

This dependence of f_M on Q_L was tested by making the experimental waveguide cavity length $\sim 3\lambda_g/2$ instead of $\sim \lambda_g/2$ and finding the maximum frequency of oscillation. This should raise Q_L by a factor of three and therefore decrease f_M by a factor of one-third. The measured result was a decrease in f_M by a factor of 0.41. This discrepancy may again have been due to not achieving the same RF conditions in the two cases.

In another test of eq. (11), the loaded cavity Q was measured after having made the bias-circuit impedance measurements necessary to determine f_M, R_{sc}, and R_- for the same microwave circuit conditions. The results were $\gamma = 113.3 \times 10^6$, $R_{sc} = 35\ \Omega$, $R_- = 119\ \Omega$ which, together with the assumption $s = 2$, give $Q_L \cong 261$. The microwave measurement yielded $Q_L \cong 268$, in good agreement.

We conclude that eq. (5) is a good representation of the terminal impedance at baseband frequencies in a large-signal IMPATT diode oscillator and that γ is well approximated by either (9) or (10).

VI. BIAS-CIRCUIT STABILIZATION

Up to this point, the major emphasis has been on characterizing the induced negative resistance and discussing its role as the cause of bias-circuit oscillations and tuning-induced burnout. We now turn our attention toward the principles and techniques of the stabilization of this negative resistance. By stabilizing we mean the achievement

of small-signal stability so that any fluctuation in bias-circuit current or voltage eventually decreases to zero. In addition to small-signal stability, we also require large-signal stability so that transients in power supply lines cannot cause instabilities to develop.

6.1 *Stability Criterion*

The stability criterion is derived by starting with the loop impedance equation

$$(Z_B + Z_t)i_B = e_n$$

where Z_B is the bias-circuit impedance, i_B the fluctuating component of current, and e_n is an assumed noise voltage. In the complex frequency plane ($s = \sigma + j\omega$), if $Z_B + Z_t$ has any zeros in the right-half plane ($\sigma > 0$), that component will grow in time, and the circuit plus diode is unstable. The Nyquist criterion is used to determine the number of zeros minus the number of poles of $Z_B + Z_t$ that are in the right-half plane. This is not so convenient here, since we are working with Z_t and Z_B as two separate sets of data and can only change the design of Z_B. We therefore consider the function $Z_Q - Z_B$, where $Z_Q = -Z_t$. This must have the same number of poles and zeros in the right-half plane. Now, however, we plot the loci of Z_Q and Z_B separately as ω goes from $-\infty$ to $+\infty$ and consider the vector pointing from $Z_B(\omega)$ to $Z_Q(\omega)$. We then see that the net number of rotations of the vector $Z_Q(\omega) - Z_B(\omega)$ indicates the number of zeros minus the number of poles in the right-half plane. In addition, since Z_B is a passive driving point impedance function, it cannot have any poles or zeros in the right-half plane. Therefore,

$$Z_Q(s) - Z_B(s) = \frac{R_-}{1 + s/\gamma} - R_{sc} - Z_B(s)$$

has no poles in the right-half plane and the number of rotations of the impedance vector $Z_Q(\omega) - Z_B(\omega)$ gives directly the number of right-half plane zeros.

To understand this in practical terms, we show schematically in Fig. 10 three conditions; stable, unstable, and conditionally stable for a typical bias circuit. The bias-circuit impedance, $Z_B(\omega)$, and the diode quenching impedance, $Z_Q(\omega)$, are separately plotted as a function of frequency over the complete frequency range for which $Z_t(\omega)$ has negative real part. The criterion then becomes: The bias circuit is stable if, at the point P where the two loci intersect, the frequency ω_{PQ} on the Z_Q locus is lower than the frequency ω_{PB} on the Z_B locus;

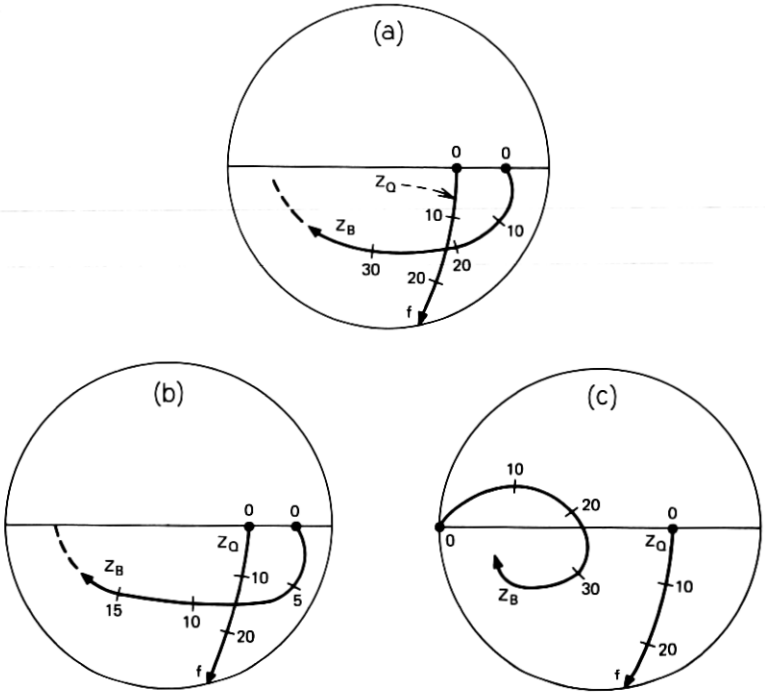

Fig. 10—Illustration of (a) stable, (b) unstable, and (c) conditionally stable bias-circuit impedance loci.

otherwise, an instability exists. In Fig. 10a, the criterion is satisfied, and the circuit is stable. In Fig. 10b, the criterion is not satisfied, and the circuit is not stable. In Fig. 10c, there is not even an intersection of Z_B with the small-signal locus Z_Q. However, $Z_B(\omega)$ does lie in the large-signal region of Z_Q (see Fig. 4), and such a condition is conditionally stable. At small-signal levels, no growing root appears, but if the excitation becomes large through some disturbance, then a large-signal instability can exist. We note that changes in the bias current or microwave loading can move Z_Q all the way down to zero impedance and therefore such a circuit configuration as shown in Fig. 10c would be almost certain to burn out the diode.

6.2 *Some Examples*

We now give some simple examples which illustrate the above criterion and shed light on some commonly used biasing schemes.

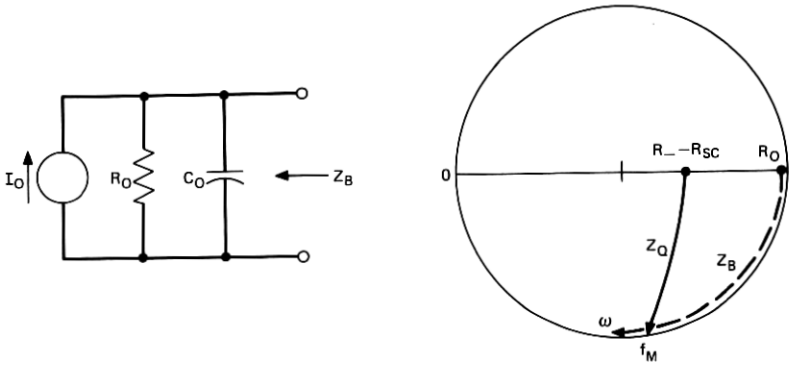

Fig. 11—Stability considerations for constant-current power supply having a lumped shunt capacitance C_o: Section 6.2.1.

6.2.1 *Constant-Current Supply—Maximum Equivalent Lumped Capacitance*

The circuit of Fig. 11a represents a constant-current supply with large shunt resistance and perhaps large shunt capacitance. Part (b) of the figure shows the impedance diagram assuming that $R_o \to \infty$. The maximum capacitance $C_{0\,\max}$ that can be tolerated before inducing instability is that which has a reactance equal to that of Z_Q at $f = f_M$, the maximum oscillation frequency. This is

$$C_{0\,\max} = \frac{1}{\gamma} \frac{1}{R_- - R_{sc}}.$$

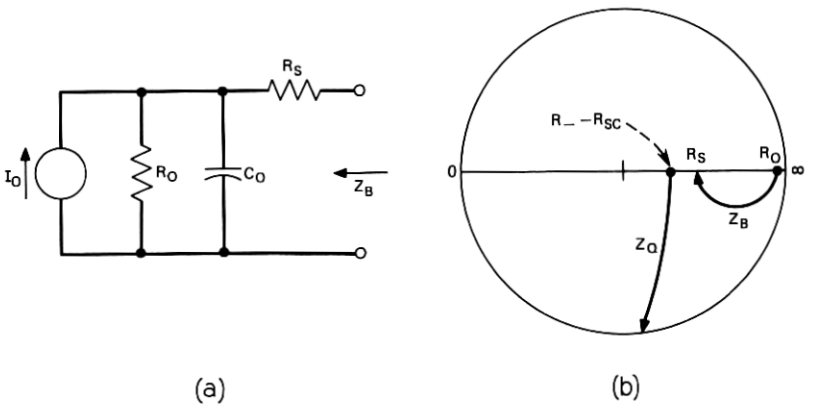

Fig. 12—Stability considerations for constant-current supply with added series resistance, R_s: Section 6.2.2.

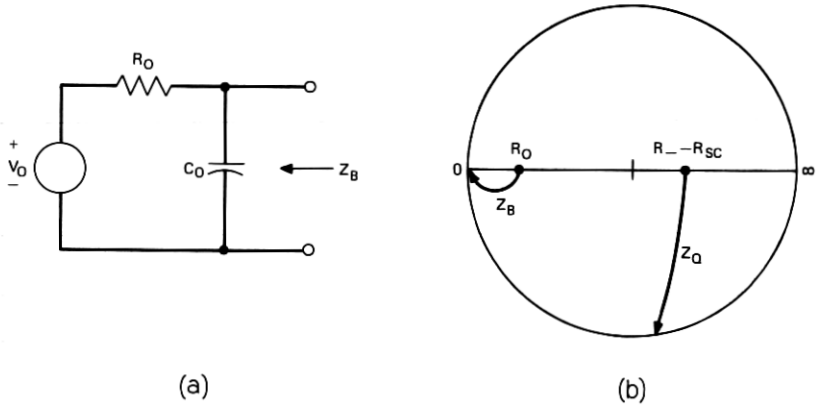

Fig. 13—Stability considerations for constant-voltage supply: Section 6.2.3.

For the GaAs oscillators used for the data in Figs. 2 and 3, we had $R_- - R_{sc} \cong 120$ ohms and $\gamma \cong 2\pi \times 10^7$ rad/s, which gives $C_{0\,\max} = 140$ pF.

6.2.2 *Constant-Current Supply—Series Resistance*

The addition of series resistance between the shunt capacitance and the diode, as in Fig. 12a, gives the impedance diagram shown in Fig. 12b. Stability is predicted for $R_s > R_- - R_{sc}$. It should be noted here that this is the easiest possible way to stabilize the bias circuit, and were it not for the large dc power dissipation incurred in R_s, this would be ideal. The larger R_s is, the larger the difference between $Z_B(\omega)$ and $Z_Q(\omega)$, and the less the noise amplification is in the bias circuit, giving less upconverted noise in the microwave spectrum.

6.2.3 *Constant-Voltage Supply*

For a constant-voltage supply, the series resistance is usually very small, and C_0 is large. Figure 13 shows the circuit and impedance diagram and we see that this is a conditionally stable circuit. As the bias current is turned up from zero, the Z_Q locus moves through the low-impedance region, and this scheme is certain to burn out diodes. The addition of a large series resistance moves the whole Z_B locus to the high-impedance region and stability is indicated again.

6.2.4 *Constant-Current Supply—Series Inductance*

The addition of a large series inductance, as shown in Fig. 14, might be thought to hold the current more constant and therefore add stability. In fact, such an addition creates a series resonance which lowers

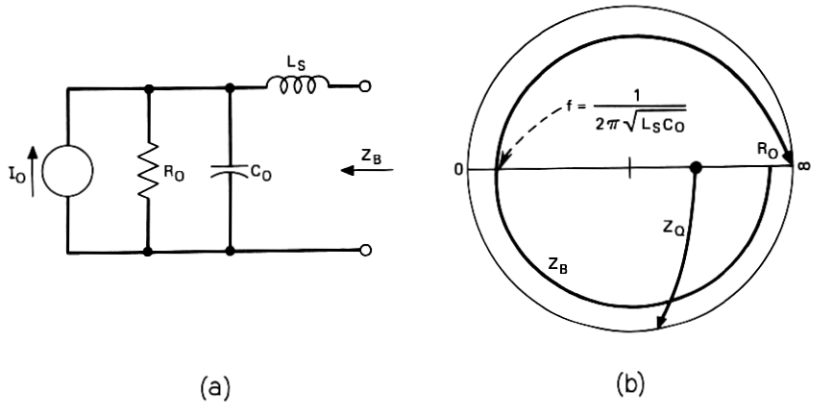

Fig. 14—Stability considerations for constant-current supply with added series inductance: Section 6.2.4.

the bias-circuit impedance at all frequencies below the resonance. Thus, the $Z_B(\omega)$ locus must intersect the $Z_Q(\omega)$ locus at a lower frequency (on Z_B), and this is in the direction of making the circuit unstable. Thus a series inductance worsens stability. Of course, some inductances have rather large series resistances, and this may, in itself, tend to improve stability.

6.2.5 *Constant-Current Supply—Resistive Choke Stabilizer*

The need to get rid of the dc loss in the stabilizing circuit forces one to consider parallel inductance-resistance networks as shown in Fig. 15. The constant-current supply is shown with parasitic shunt capacitance C_0 and series resistance R_s. R_s must be greater than $R_- - R_{sc}$ for this scheme to work, but it is used only to stabilize the lower frequency range, and may therefore be put further from the diode. Between R_s and the diode, there is additional shunt capacitance denoted by C_1. To stabilize the effects of C_1, a parallel inductance-resistance network can provide the locus Z_B shown (approximately) and therefore stabilize the oscillator. A simple design criterion may be formulated by assuming R_s to be very large. By choosing L/R large enough, the locus of Z_B may be made to resemble that of the pure series resistance, shunt capacitance case as closely as desired. From a graphical evaluation, the criterion $L \approx 3C_1R^2$ together with $R = 2$ to 5 times $R_- - R_{sc}$ gives an adequate margin of stability. For the GaAs oscillator circuit, an experimental model of this choke was made with $R = 470$ ohms, and $L = 75\,\mu$H. This would satisfy the above criterion for a capacitance

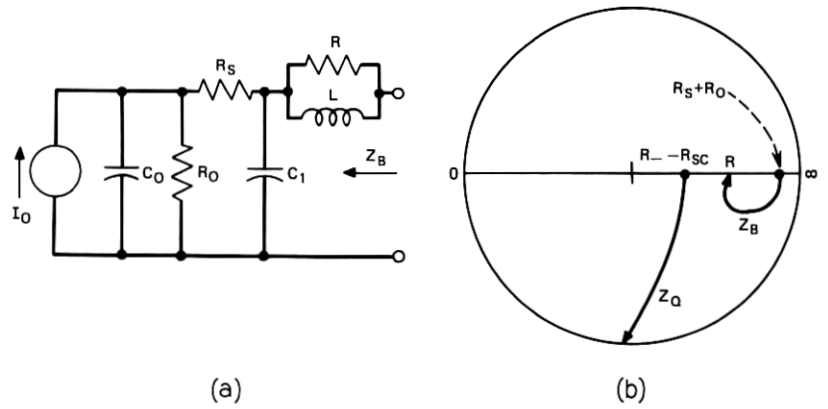

Fig. 15—Stability considerations for constant-current supply with resistive choke stability network: Section 6.2.5.

of 100 pF. In actual fact, it was possible to make $C_1 = 3000$ pF without causing instability. With $C_1 = 10{,}000$ pF, the diode burned out. The technique used to construct the choke is illustrated in Fig. 16. The body of the choke is made of a ferrite material similar to that used in low-frequency inductors. A hole is drilled through the center and a 470-ohm $\frac{1}{8}$-watt carbon resistor inserted. The winding around the ferrite is made of three layers of number 35 FORMVAR wire. Attached

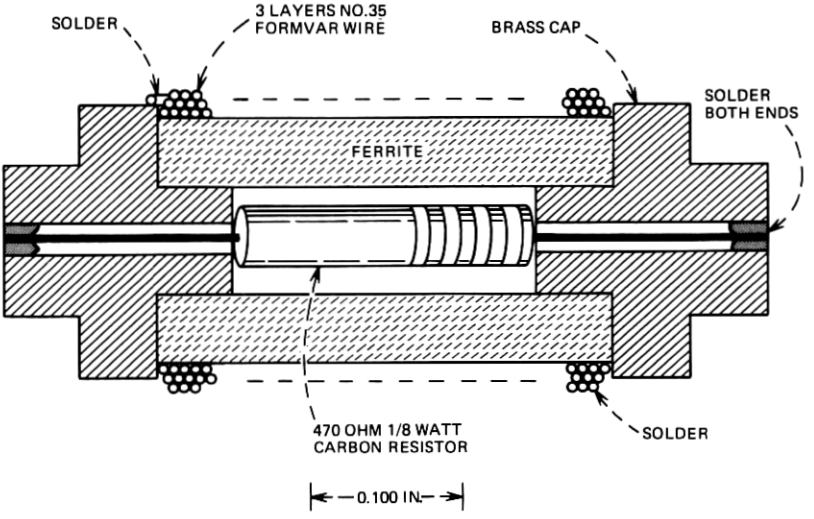

Fig. 16—Mechanical construction of the resistive choke stabilizing network.

to the ends are brass caps which thread into the center conductor of the coaxial bias line. This choke is placed at the same position indicated for R_s in Fig. 1. A broader bandwidth might be achieved by lowering the resistance and inductance values, with some sacrifice of stability margin.

In the particular model built, no attempt was made to insure low reflections at microwave frequencies from the bias circuit when the choke was inserted. It would be desirable to do this for a practical oscillator.

With this resistive choke stabilizing network, a GaAs IMPATT oscillator was made to give 3.4 watts of output power with 12 percent efficiency at 250 mA bias current. Without any stabilization, diodes of this same type (breakdown capacitance $\sim$2.5 pF, breakdown voltage $\cong$105 volts) consistently burned out at 80 to 100 mA. This network has vastly improved the stability of the bias circuit, but provides lossless dc power transmission from the constant-current supply to the diode.

Using a more sophisticated biasing network, designed upon the criteria developed here, but which provides a more controlled impedance locus than achievable with a simple RL choke, it has been possible to stabilize the bias circuit over all current ranges up through thermal burnout of the diode, without loss of RF or dc power.

A word of warning about the general use of chokes for stabilization: if the inductance is not large enough, such a choke actually worsens the instability and hastens burnout.

6.2.6 *Bias-Circuit Line Length*

In the previous examples it has been assumed that the terminations specified were all positioned exactly at the diode. In fact, this cannot be true and, therefore, a finite length of transmission line is necessary between the diode and the termination. This effect causes the termination impedance to be transformed to a lower impedance, and increases the likelihood of an instability. This places a limit on the length of line that can be tolerated between the diode and the stabilizing network. For example, for the GaAs data of Fig. 2, and a pure stabilizing resistance of 500 ohms, the maximum length of line is about $l_{max} = 0.09\,\lambda$ at a frequency of about 13 MHz. But $\lambda = c/(f\sqrt{\epsilon_r})$, where ϵ_r is the dielectric constant of the material in the bias line. This gives about 2 meters for air line with $\epsilon_r = 1$. In common microwave absorbent materials such as Eccosorb MF 124, $\epsilon_r = 27$ and l reduces to 40 cm. This is for a medium Q oscillator, Q_L being $\sim$250. For a low-Q

oscillator ($Q_L \sim 25$) the frequencies all will scale with $1/Q$ so the line length then reduces (in the Eccosorb material) to ~4 cm, which is beginning to be difficult to do.

If the termination is frequency dependent, the effect of line length can be more pronounced. An example, a length l of transmission line terminated in a pure capacitance, is illustrated in Fig. 17. Since at $f = f_M$, $X_Q/Z_o = -1.3$ for the GaAs oscillator (see Fig. 2), the frequency at which $X_B/Z_o = -1.3$ gives the maximum f_M tolerable without initiating bias instabilities for each value of C. This value of f_M is plotted versus C for $l = 10$, 20, and 30 centimeters, and may be used to derive either (*i*) the maximum value of shunt capacitance, (*ii*) the maximum length l for a given C and f_M, or (*iii*) the smallest value of microwave loaded Q [eq. (11)], which is tolerable before oscillation or instability occurs. For example, with a capacitance

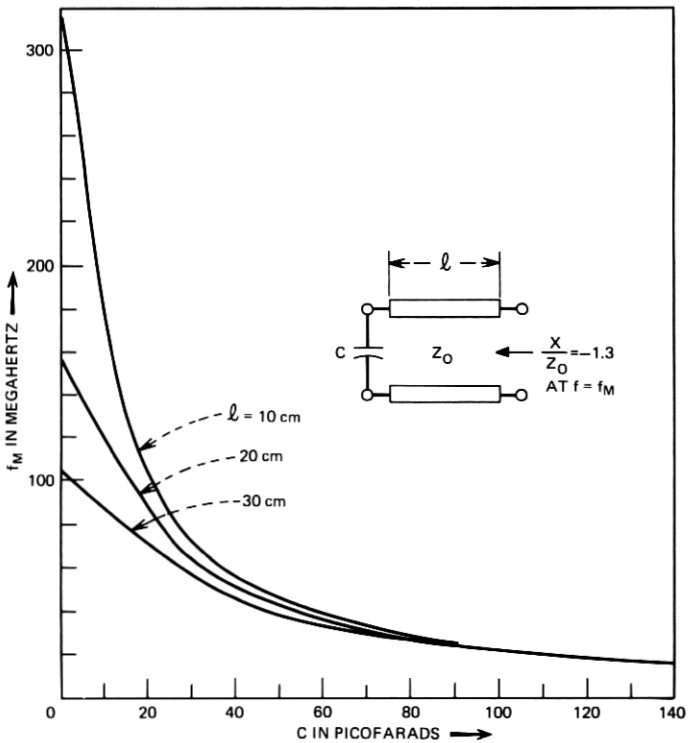

Fig. 17—Depicting the effect of a length of line, l, between the diode (having maximum bias-circuit oscillation frequency f_M) and a shunt capacity C, for the GaAs diode terminal impedance shown in Fig. 2.

$C = 50$ pF, $f_o = 6$ GHz, $l = 10$ cm, and $R_-/R_{sc} = 4.3$ we find $f_M \cong 47$ MHz and $Q_L = 232$. Thus the loaded Q would have to be greater than 232 in order that a 50-pF shunt capacitance at a distance of 10 cm from the diode would not cause instability in a 6-GHz GaAs oscillator similar to those used in these experiments.

6.2.7 *Higher-Impedance Bias Circuits*

If the bias-circuit characteristic impedance were made several times larger than the maximum induced value of negative resistance, then a matched termination at all frequencies would insure stable operation. Even small reflections could easily be tolerated, regardless of their distance from the diode. The difficulty with this is that it is very difficult to make good circuits with very-high-impedance lines. Traditionally, 50 ohms is used. Any increase above that value would materially assist the stabilization of the bias circuit. On the other hand, one could also decrease the impedance of the diode by making its area larger. In either case, difficulty will eventually be encountered because of the problem of matching the diode to the microwave circuit, but it is probable that some gain over the present situation can be had by these techniques.

VII. SCALING LAWS

The negative resistance of eq. (2) is obviously a function of the diode area and length, the maximum field strength, and the avalanche coefficient. It is therefore reasonable to inquire as to how R_- scales with different oscillator designs, material, and frequency. This can be worked out rather simply for the Read diode model assumed here, but for abrupt junction pn diodes this model fails to answer the question, how should the design of the diode be changed to decrease the value of R_-, while still achieving high-power, high-efficiency microwave operation?

For the Read diode, in the large-pulse approximation we may assume the negative conductance is approximately

$$g_d = -\frac{4}{\pi}\frac{I_d}{V_a}.$$

Then

$$\frac{dV_a}{dI_d} = -\frac{\left(\frac{\partial g_d}{\partial I_d}\right)_{V_a}}{\left(\frac{\partial g_d}{\partial V_a}\right)_{I_d}} = \frac{V_a}{I_d}.$$

Therefore,

$$\frac{I_d}{V_d}\frac{dV_a}{dI_d} = \frac{V_a}{V_d} \equiv \delta,$$

δ being the normalized ac voltage amplitude and V_d the breakdown voltage of the diode. The ratio δ is assumed here, as elsewhere,[14] to be invariant with frequency scaling, and with this assumption we find that R_- for a new, optimally designed diode, as compared with R_{-o} for a reference diode, is given by

$$\frac{R_-}{R_{-o}} = \left(\frac{m}{m_o}\right)\cdot\left(\frac{V_d}{V_{do}}\right)\cdot\left(\frac{I_{do}}{I_d}\right) = \left(\frac{m}{m_o}\right)\cdot\left(\frac{Z_d}{Z_{do}}\right). \tag{12}$$

Here Z_d is defined as the ratio of the breakdown voltage to the operating current and $W\cdot E_c$ has been set equal to V_d.

An interesting application of (12) is to the millimeter-wave Si IMPATTs designed to work at 100 GHz. For these diodes $V_d \cong 13$ volts, and a typical current is 0.1 ampere, giving $Z_d = 130$ ohms. For typical 6-GHz Si IMPATTs $V_d = 105$ volts, and a typical current is 0.20 ampere, giving $Z_{do} = 525$ ohms. Therefore,

$$\frac{R_-(\text{100-GHz diode})}{R_{-o}(\text{6-GHz diode})} \cong \left(\frac{m}{m_o}\right) \times 0.25.$$

It is found that R_{-o} is a few ohms and that $m/m_o < 1$, so it is predicted that the millimeter-wave IMPATT diodes should have very small induced negative resistance.

VIII. SUMMARY AND CONCLUSIONS

In this paper we have shown that a low-frequency negative resistance is induced in the IMPATT diode by the large-signal characteristics of the oscillator. This low-frequency negative resistance has been shown to be responsible for both bias-circuit oscillations and a class of low-current burnouts, normally called "tuning-induced" burnouts. The large upconversion of noise that often occurs is also caused by this same effect.

The origin of the negative resistance was shown to be the combination of the rectification property of the nonlinear ac avalanche, the coupling of fluctuations in the bias current to fluctuations in the microwave voltage amplitude by the microwave circuit oscillator constraint, and the fact that increases in the microwave voltage amplitude and dc bias current generally drive the large-signal microwave admittance of the diode in opposite directions on the admittance

plane. Calculations were made showing the correctness of this picture, and were applied to Si, Ge, and GaAs diodes designed for 6-GHz operation. The agreement with experimental results is good, showing a small value of negative resistance for Si (typically less than 10 ohms), somewhat larger for Ge (typically 35 to 75 ohms), and larger yet for GaAs (typically 85 to 150 ohms).

A reasonably complete experimental characterization of this negative resistance was given, showing its dependence on baseband frequency, dc bias current, and microwave loading conditions. It was found that, at low enough bias currents, the negative resistance was small for microwave loads near those which gave maximum power. At higher bias currents, however, the negative resistance approached its maximum value at or near optimum loading conditions. It was also found that the negative resistance had a low-pass frequency characteristic and an inductive reactance associated with it. The negative resistance was found to go to zero at a frequency called f_M, the theoretical maximum frequency of oscillation, and f_M was found experimentally to be roughly inversely proportional to the microwave circuit's loaded Q factor. It was found that, for large-signal bias-circuit oscillations, the negative resistance decreased, and the reactance remained approximately constant. This fact indicates open-circuit stability, and is very important in the stabilization of the bias circuit.

An analysis was performed and an equivalent circuit was derived, showing that the inductive reactance observed experimentally is best represented by a negative capacitance, $-1/\gamma R_-$, in parallel with the negative resistance, $-R_-$, all in series with the space-charge resistance, R_{sc}. This circuit predicts several aspects of the small-signal behavior of the induced negative resistance, and allows the stabilization techniques to be designed in a straightforward manner. The agreement of this equivalent circuit with the experimental results is good and it shows in detail how the interaction of the microwave circuit and diode admittances affect the low-frequency negative resistance. In particular, it is shown that the maximum frequency of oscillation, f_M, is given by

$$f_M = \frac{f_o}{Q_L}\sqrt{\frac{R_-}{R_{sc}} - 1}$$

where f_o is the microwave frequency of oscillation, Q_L is the loaded Q of the microwave cavity, R_{sc} is the space-charge resistance of the diode, and $R_- - R_{sc}$ is the low-frequency asymptote of the negative resistance. Smith chart plots of the negative of the diode's small-signal terminal impedance, $(-)Z_t$, are given for various values of

R_-/R_{sc} and normalized frequency. The shape of these loci is found to vary somewhat, though not drastically, with the choice of impedance normalization used. When normalized to 50 ohms (which is greater than R_{sc}), the contours always appear somewhat as shown in Fig. 2.

Stabilization techniques were discussed, beginning with the development of a simple means of judging the stability of a given oscillator and bias circuit. Several examples of stable and unstable conditions were given including:

(*i*) a calculation of the maximum equivalent lumped shunt capacitance that can still remain stable,

(*ii*) discussion of the effects of line length in the bias circuit which indicated the desirability of placing any stabilization network as close to the diode as possible, but at the same time indicating that it need not be exactly at the diode,

(*iii*) a stabilizing network consisting of a pure series resistance, R_s, in the bias circuit with $R_s \gg R_- - R_{sc}$ (it is required that there be no significant reactance or line length between the diode and R_s), and

(*iv*) an alternative stabilizing network consisting of a parallel inductance-resistance choke combination that does not dissipate dc power.

Using the principles of stabilization outlined here, it has been possible to stabilize the bias circuit of IMPATT oscillators over the full range of bias currents up to the diode's thermal burnout limit.

As a final topic, the frequency scaling of R_- was considered, and it was shown as an example that the 100-GHz Si IMPATTs should have very small induced negative resistances, and therefore the instabilities encountered at lower frequencies and in Ge and GaAs should not be a serious problem for the millimeter-wave Si diodes.

IX. ACKNOWLEDGMENTS

The author wishes to thank F. M. Magalhaes for early experimental contributions leading to the success of this investigation, and for providing the microwave oscillator circuits used in all of the experiments. The author also thanks K. Kurokawa for general guidance and especially for suggestions leading to the development of the equivalent circuit. The GaAs diodes were supplied by J. C. Irvin and D. J. Coleman, who first brought to the author's attention the severity of the problem in GaAs. The Si and Ge diodes were supplied by D. R. Decker and C. N. Dunn. Thanks also go to R. S. Riggs who performed a good many of the experiments reported here.

APPENDIX

It is the purpose of this Appendix to derive the equivalent circuit of the low-frequency diode impedance of an IMPATT diode oscillator. To do this, the Read diode model is assumed to describe the diode and a quasi-static technique is assumed to describe its interaction with the microwave circuit. Rewriting eqs. (8) and (9) of Kurokawa's work[11] to apply to admittance, and dropping the noise voltage terms, we may write

$$[G(\omega) - g]B'(\omega) - [B(\omega) + b]G'(\omega) + |Y'(\omega)|^2 \frac{1}{V_a}\frac{dV_a}{dt} = 0 \quad (13)$$

$$[G(\omega) - g]G'(\omega) + [B(\omega) + b]B'(\omega) + |Y'(\omega)|^2 \frac{d\varphi}{dt} = 0. \quad (14)$$

Here, $Y(\omega) = G(\omega) + jB(\omega)$ is the microwave circuit admittance, $y = -g + jb$ is the device admittance, V_a and φ are the microwave voltage amplitude and phase, and are assumed to be slowly varying functions of time, and the prime on G, B, and Y denotes differentiation with respect to frequency. Equations (13) and (14) describe the change in time of the amplitude and phase of a negative conductance oscillator. In steady-state oscillation, $dV_a/dt = 0$ and $d\varphi/dt = 0$, implying

$$G(\omega) - g(V_a,I) = 0, \quad (15)$$

and

$$B(\omega) + b(V_a,I) = 0, \quad (16)$$

which determine the steady-state oscillation amplitude A_o and frequency ω_o. We have assumed that g and b are independent of frequency, which only implies that the analysis is restricted to situations in which $Y(\omega)$ varies much more rapidly than y.

Let us now presume that the steady-state amplitude and bias current are perturbed by a small amount, that is

$$I_d = I_o + \Delta I$$

and

$$V_a = A_o + A_o\delta$$

where $\Delta I \ll I_o$ and $\delta \ll 1$. Then, linearizing the variation of g and b with both V_a and I_d gives

$$g = G - sG\delta + k_g\Delta I$$

and

$$b = -B + rG\delta - k_b\Delta I$$

where

$$s = -\frac{A_o}{G}\frac{\partial g}{\partial V_a}, \qquad r = \frac{A_o}{G}\frac{\partial b}{\partial V_a}$$
$$k_g = \frac{\partial g}{\partial I}, \qquad k_b = -\frac{\partial b}{\partial I} \tag{17}$$

are the RF voltage and dc current linearization parameters of the diode's admittance, evaluated at the steady-state large-signal oscillation point. We may then write

$$[sG\delta - k_g\Delta I]B' - [rG\delta - k_b\Delta I] + |Y'|^2\frac{d\delta}{dt} = 0.$$

Collecting terms,

$$\frac{d\delta}{dt} + \gamma\delta = \Delta f \tag{18}$$

where

$$\gamma = \frac{sGB' - rGG'}{G'^2 + B'^2} \tag{19}$$

and

$$\Delta f = \frac{B'k_g - G'k_b}{G'^2 + B'^2}\Delta I. \tag{20}$$

Introducing

$$G'/B' = \tan\theta_c,$$
$$r/s = \tan\theta_d,$$

and

$$\theta = \theta_c + \theta_d + \pi/2,$$

we obtain

$$\gamma = \frac{\sqrt{r^2 + s^2}}{\left|\frac{\partial Y}{\partial\omega}\right|} G\sin\theta, \tag{21}$$

which is eq. (7) of the text.

Equation (19) for Δf becomes

$$\Delta f = \frac{\sqrt{k_g^2 + k_b^2}}{\left|\frac{\partial Y}{\partial\omega}\right|}\sin(\chi)\Delta I. \tag{22}$$

The meaning of the angles θ_c, θ_d, and θ can be seen in Fig. 18 where it is seen that θ is the total angle of intersection between the negative of the circuit admittance curve, and the tangent to the large-signal

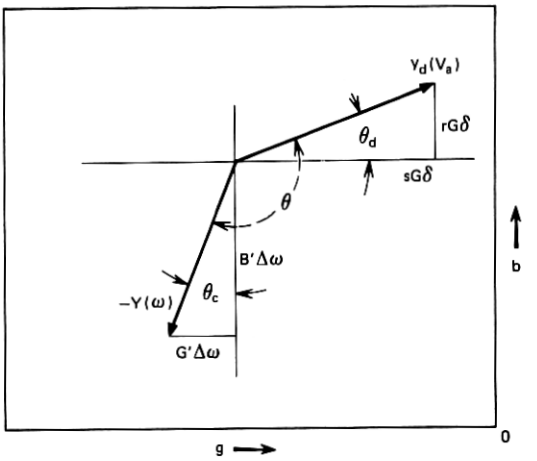

Fig. 18—Defining the angles θ_c, θ_d, and θ in the microwave large-signal admittance plane of the diode.

device variation with voltage amplitude, at the steady-state operating point. The angle χ is defined by

$$\chi = \frac{\pi}{2} - \theta_I - \theta_c$$

with θ_c defined as above and θ_I defined by

$$\tan \theta_I = \frac{k_b}{k_g}.$$

The graphical interpretation of χ is given by Fig. 19, and it is seen to be the angle between the negative of the circuit admittance and the direction of the variation of the large-signal device admittance with dc current, also at the steady-state operating point.

Assuming an $\exp(j\omega t)$ time dependence for δ and ΔI, that is $\delta = \text{Real}(\tilde{\delta} e^{j\omega t})$, and $\Delta I = \text{Real}(\tilde{\imath}_m e^{j\omega t})$, eq. (17) gives

$$\tilde{\delta} = \frac{\widetilde{\Delta f}}{\gamma(1 + j\omega/\gamma)}$$

or

$$\tilde{\delta} = \frac{\sqrt{k_g^2 + k_b^2}}{\sqrt{r^2 + s^2}} \frac{\sin \chi}{\sin \theta} \frac{1}{G} \frac{\tilde{\imath}_m}{(1 + j\omega/\gamma)}.$$

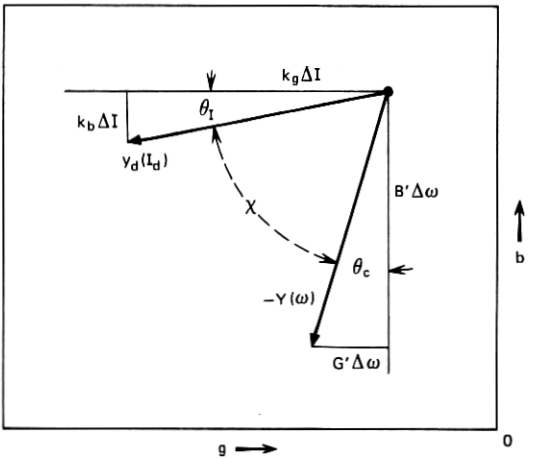

Fig. 19—Defining the angles θ_I, θ_c, and χ in the microwave large-signal admittance plane of the diode.

But

$$\frac{\sqrt{k_g^2 + k_b^2}}{\sqrt{\gamma^2 + s^2}}\left(\frac{A_o}{G}\right) = \frac{\left|\frac{\partial y}{\partial I_d}\right|}{\left|\frac{\partial y}{\partial V_a}\right|} = \left|\frac{dV_a}{dI_d}\right|$$

so

$$\tilde{\delta} = \frac{1}{A_o}\frac{\sin\chi}{\sin\theta}\left|\frac{\partial V_a}{\partial I_d}\right|\frac{\tilde{\imath}_m}{(1 + j\omega/\gamma)}.$$

We may therefore interpret γ as the modulation frequency at which the microwave power in the sideband ($\sim|\delta|^2$) is one-half of its low-frequency response, that is, the common 3-dB modulation half-bandwidth of the oscillator.

The rectification equation, eq. (1) of the text, is now assumed to be true as V_a varies slowly with time. This gives, for the voltage at frequency ω (to first order in $\tilde{\delta}$),

$$\tilde{V}_m = R_{sc}\tilde{\imath}_m - \frac{m}{4W\epsilon_c}2V_a^2\tilde{\delta}$$

or

$$Z_t = \frac{\tilde{V}_m}{\tilde{\imath}_m} = R_{sc} - \frac{m}{4W\epsilon_c}\frac{\sin\chi}{\sin\theta}\left|\frac{dV_a^2}{dI_d}\right|\frac{1}{(1 + j\omega/\gamma)}. \qquad (23)$$

We may then write

$$Z_t = R_{sc} - \frac{R_-}{1 + j\omega/\gamma} \tag{24}$$

where R_- and γ are defined by eqs. (6) and (7) of the text. Z_t is the terminal impedance of the diode at baseband frequencies, and if $R_- > R_{sc}$, then a net negative resistance exists at low frequencies. The equivalent circuit for Z_t is shown in Fig. 7 and its properties are discussed in Section V of the text.

REFERENCES

1. Clorfeine, A. S., and Hughes, R. D., "Induced dc Negative Resistance in Avalanche Diodes," Proc. IEEE (Letters), *57*, No. 5 (May 1969), pp. 841–842.
2. Olson, H. M., Jr., "Negative Resistance Diode Coaxial Oscillator with Resistive Spurious Frequency Suppressor," U. S. Patent No. 3,621,463, November 16, 1971.
3. "Microwave Power Generation and Amplification using IMPATT Diodes," Hewlett-Packard Application Note 935, Hewlett-Packard Corp., Palo Alto, California.
4. Read, W. T., Jr., "A Proposed High-Frequency, Negative Resistance Diode," B.S.T.J., *37*, No. 3 (March 1958), pp. 401–446.
5. Evans, W. J., Scharfetter, D. L., Johnston, R. L., and Key, P. L., "Tuning Initiated Failure in Avalanche Diodes," J. Appl. Phys., *42*, No. 2 (February 1971), pp. 799–803.
6. Blue, J. L., "Approximate Large-Signal Analysis of IMPATT Oscillators," B.S.T.J., *48*, No. 2 (February 1969), pp. 383–396.
7. Sze, S. M., *Physics of Semiconductor Devices*, New York: John Wiley and Sons, 1969.
8. Gewartowski, J. W., and Morris, J. E., "Active IMPATT Diode Parameters Obtained by Computer Reduction of Experimental Data," IEEE Trans. Microwave Theory and Techniques, *MTT-18*, No. 3 (March 1970), pp. 157–161.
9. Magalhaes, F. M., and Kurokawa, K., "A Single-Tuned Oscillator for IMPATT Characterizations," Proc. IEEE (Letters), *58*, No. 5 (May 1970), pp. 831–832.
10. Gupta, M. S., "Noise in Avalanche Transit-Time Devices," Proc. IEEE, *59*, No. 12 (December 1971), pp. 1674–1687.
11. Kurokawa, K., "Some Basic Characteristics of Broadband Negative Resistance Oscillator Circuits," B.S.T.J., *48*, No. 6 (July–August 1969), pp. 1937–1955.
12. Scharfetter, D. L., and Gummel, H. K., "Large-Signal Analysis of a Silicon Read Diode Oscillator," IEEE Trans. Electron Devices, *ED-16*, No. 1 (January 1969), pp. 64–77.
13. Kurokawa, K., "Noise in Synchronized Oscillators," IEEE Trans. Microwave Theory and Techniques, *MTT-16*, No. 4 (April 1968), pp. 234–240.
14. Scharfetter, D. L., "Power-Impedance-Frequency Limitations of IMPATT Oscillators Calculated from a Scaling Approximation," IEEE Trans. Electron Devices, *ED-18*, No. 8 (August 1971), pp. 536–543.